Received: 10 May 2021 | Revised: 21 April 2022 | Accepted: 13 June 2022

DOI: 10.1111/jfr3.12833

ORIGINAL ARTICLE

CIWEM Chartered Institution of Water and Environmental Management | Journal of Flood Risk Management | WILEY

Potential for seasonal flood forecasting in West Africa using climate indexes

Jean Hounkpè[1] | **Bruno Merz**[2] | **Félicien D. Badou**[3] | **Aymar Y. Bossa**[1] | **Yacouba Yira**[4] | **Emmanuel A. Lawin**[1]

[1]National Water Institute, University of Abomey Calavi, Abomey Calavi, Atlantic, Benin

[2]Helmholtz Centre Potsdam, German Research Centre for Geosciences (GFZ), Section Hydrology, Potsdam, Germany

[3]Ecole d'Horticulture et d'Aménagement des espaces Verts, Université Nationale d'Agriculture, Kétou, Benin

[4]Applied Science and Technology Research Institute–IRSAT/CNRST, Ouagadougou, Burkina Faso

Correspondence
Jean Hounkpè, National Water Institute, University of Abomey Calavi, Abomey Calavi, BP 2008 Abomey Calavi, Benin.
Email: jeanhounkpe@gmail.com

Funding information
Bundesministerium für Bildung und Forschung, Grant/Award Number: ClimapAfrica Program

Abstract

Floods are among the most devastating natural disasters and are expected to become more severe with changing climate and population growth. Flood forecasting is one of the key components of flood risk reduction. The potential for seasonal flood forecasting through climate indexes has not been studied for West Africa so far. This work investigates how climate indicators can be used to predict in advance, one to several months ahead of the flood season, above or below normal flood discharge in West Africa. Six global and regional climate indexes were screened for their potential to predict flood discharge of 56 river gauging stations across West Africa. Forecasting models are developed, based on simple and multiple linear regressions between climate indexes and annual maximum discharge, and evaluated using the relative operating characteristics and the relative operating levels scores. The western dipole mode index is the most skillful individual climate index for above normal flood prediction. Combining climate indexes via multiple linear regressions outperforms individual climate indexes for both above and below normal flood prediction. The models show forecasting skills for up to 4 months prior to the flood season. Hence, this study opens promising possibilities for seasonal flood forecasting in West Africa. This may help alert disaster reduction agencies of entering a period of an increased chance of flooding and may trigger adequate mitigation measures.

KEYWORDS

climate indexes, flood occurrence, seasonal flood forecasting, teleconnection, West Africa

1 | INTRODUCTION

Climate change and its associated increase in the intensity and frequency of hydrological extremes such as floods is one of the current global challenges (Dottori et al., 2018; Merz et al., 2021). Disaster risk reduction (DRR), and particularly flood DRR (FDRR), supports communities to adapt to the negative impacts of climate change and remains of primary importance in achieving sustainable development goals (SDGs).

A key component of FDRR is flood preparedness, which requires prior knowledge of flood intensity and

frequency to shape appropriate responses. Seasonal forecasting of flood frequency and quantiles, several months ahead, could be valuable information for enhanced preparedness in flood risk management. However, its potential is largely unexplored (Arnal et al., 2018). In Africa, several initiatives have been undertaken to forecast floods (Thiemig et al., 2011). However, these initiatives focus on lead times varying between 1 and 15 days, emphasizing short-term flood forecasting of lead times up to 3 days.

The potential benefit of flood forecast information increases with the lead time. Therefore, with at least 1 month of lead time, seasonal flood forecasting could substantially improve flood risk management strategies. This time could be used to release water from dams to provide additional retention capacity or to procure disaster management supplies and implement strategies (White et al., 2017). Seasonal forecasts cannot predict the weather or the flood peak at a certain point in space or time. However, they inform about probable anomalies and deviations from the normal or average conditions, for instance, shifts in flood probability distribution (White et al., 2017). This predictability is driven mainly by slowly varying Earth system components, such as sea surface temperature (SST). Hence, flood peak distributions are often related to large-scale circulation patterns (Kundzewicz et al., 2019) like el nino southern oscillation (ENSO). Evidence of such a relation was given by Ward, Jongman, et al. (2014) who examined correlations between observed peak discharge and the southern oscillation index (SOI) on the global scale. They found strong relationships between ENSO and annual floods in most parts of the globe. There is also evidence from a substantial number of regional studies. For example, Räsänen and Kummu (2013) found that ENSO significantly influenced the hydrology of the Mekong River and that flood duration was on average more than 1 month longer during La Niña years compared to El Niño years. The stratification of a regional flood index according to ENSO and interdecadal pacific oscillation led to marked differences in flood quantiles for 40 flood gauges in New South Wales, Australia (Kiem et al., 2003). Steirou et al. (2019) detected coherent spatial patterns and substantial associations between climate indexes and flood probabilities across Europe. Nakamura et al. (2013) showed that 20 major flood events in the Ohio River basin over the last 100 years had nearly identical storm tracks, moisture source, and delivery patterns suggesting that major flood events are caused by specific large-scale climate patterns. Similarly, Hounkpè et al. (2015) found a strong and statistically significant relationship between the annual maximal discharge in the Ouémé basin (Benin) and climate indexes, such as the sea level pressure (SLP) and SST of the Gulf of Guinea. Further, associations between climate indexes and flood damage have been identified for Europe (Zanardo et al., 2019) and at the global scale (Ward, Jongman, et al., 2014). A promising research path would be to use the potential predictability of climate indexes such as ENSO to provide estimates of flood hazard with lead times up to several months (Ward, Eisner, et al., 2014; Ward, van Pelt, et al., 2014).

To the best of our knowledge, no attempt has been made so far to estimate annual maximal discharge based on climate indexes for seasonal flood forecasting purposes in West Africa. Therefore, the objective of this work is to investigate the link between flood quantiles and climate indexes and how this knowledge can be used to forecast flood quantiles at the seasonal scale for improved flood preparedness in West Africa.

2 | DATA AND METHODOLOGY

The methodological framework is summarized in Figure 1. Each part of the framework is described in the following sections.

2.1 | Data and data screening

Daily river discharges were obtained from the Global Runoff Database Center (GRDC) and some West African national hydrometeorological services. Six monthly climate indexes were selected including (i) tropical southern atlantic (TSA/SST) index and (ii) tropical northern atlantic (TNA/SST) index (NOAA, 2020). TNA/SST is the anomaly of the average monthly SST from 5.5 to 23.5 N and 15 to 57.5 W, while TSA/SST is the anomaly from the Equator to 20S and 10E to 30 W (Enfield et al., 1999). The choice of TNA/SST and TSA/SST was guided by the findings of Atiah et al. (2020) in which extreme precipitation in Ghana, West Africa, was found to be significantly correlated with Atlantic Ocean SST. (iii) SLP anomaly of the SOI (SOI/SLP) at Darwin and Tahiti (NOAA, 2021) was used, as well as the (iv) ENSO Nino3.4/SST (CPC/NOAA, 2005) corresponding to the SST anomaly in Nino 3.4 region (5 N-5S, 120-170 W). The (v) dipole mode index (DMI/SST) and (vi) Western DMI (DMI_West/SST) derived from the SST of the equatorial Indian Ocean (Smith, 2020) were also considered. DMI/SST is the anomalous SST gradient between the western equatorial Indian Ocean (50E-70E and 10S-10N) and the southeastern equatorial Indian Ocean (90E-110E and 10S-0N). Significant changes in flood timing between positive and negative phases of both Indian Ocean Dipole and El Niño–Southern Oscillation were found in Sub-Sahara Africa (Ficchì & Stephens, 2019).

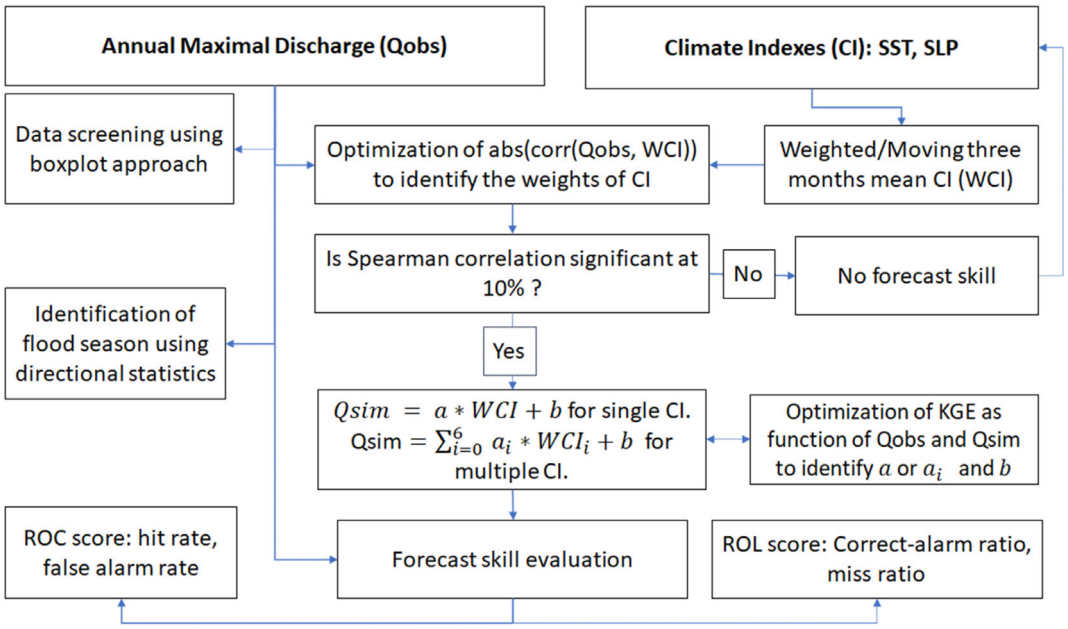

FIGURE 1 Methodological framework for seasonal flood forecasting. WCI stands for weighted mean climate index, Qsim and Qobs refer to simulated and observed flood peak discharge, respectively. KGE is the Kling and Gupta efficiency, abs, and corr represent the absolute value and correlation functions. ROC and ROL are relative operating characteristics and the relative operating levels (ROL), respectively

The block maxima approach (BMA) over the calendar year was used to obtain flood time series from continuous discharge data. To address the issue of missing data, the period of extraction of the annual maximal discharge was limited to the rainfall season, which spans generally from June to mid-November in West Africa. The boxplot approach was used to identify possible outliers due to missing data in the flood time series following the approach of Chambers et al. (2018). For any given station, after computing the interquartile range $IQR = Quantile(0.75) - Quantile(0.25)$, the lower adjacent value of the boxplot defined as the smallest value greater or equal to $Quantile(0.25) - 1.5 * IQR$ is identified. Values below the lower adjacent value are considered possible outliers due to missing data and are particularly examined with the neighboring values.

2.2 | Identification of flood season

A widely accepted method for identifying the timing of hydrological extreme events, e.g. annual maximal discharge and peak over threshold discharge, is directional statistics (Aguilar et al., 2017, Blöschl et al., 2017). Based on Bayliss and Jones (1993), the date of occurrence of an extreme event i can be transformed into directional statistics by converting the day number DN_i (varying between 1 and 366) into an angular measure θ_i:

$$\theta_i = DN_i \frac{2\pi}{365}, \tag{1}$$

Each date of occurrence can then be written in polar coordinates employing a vector with a unit magnitude and the direction specified by Equation 2. The coordinates x_m and y_m of the mean of a sample of n dates of occurrence can be written as:

$$x_m = \frac{1}{n}\sum_{i=1}^{n} cos(\theta_i) \text{ and } y_m = \frac{1}{n}\sum_{i=1}^{n} sin(\theta_i), \tag{2}$$

In polar coordinates, the mean of the sample will have the following characteristics:

$$\overline{\theta} = arctan\left(\frac{y_m}{x_m}\right) \text{ and } r = \sqrt{{x_m}^2 + {y_m}^2}, \tag{3}$$

with $\overline{\theta}$ the direction and r the magnitude of the mean of the sample. The direction $\overline{\theta}$ needs to be adjusted depending on its sign. 2π is added to negative $\overline{\theta}$ while π is added to positive $\overline{\theta}$ to limit its variation to the interval $[0, 2\pi]$. The direction $\overline{\theta}$ provides a measure of the mean timing of the event for the sample of dates and can be converted back to a mean number of days MND:

$$MND = \overline{\theta}\frac{365}{2\pi}, \tag{4}$$

The *MND* was considered in week number of the year as well as the associated standard deviation.

2.3 | Relationship between annual maximal discharge and climate indexes

Three-monthly weighted means (JFM = January to March, FMA = February to April, MAM = March to May, AMJ = April to June, MJJ = May to July) of the climate index series were computed. The weight $\alpha_{i,j,m}$ applied to m^{th} participating member ($m = 1\ to\ 3$) was obtained by optimizing the correlation between the observed annual maximal discharge of the k^{th} station ($Qobs_k$, $k = 1\ to\ 56$) and the three-monthly weighted mean climate index series $\mathrm{WCI}_{i,j}$ of the i^{th} climate index ($i = 1\ to\ 6$) and the j^{th} period ($j = 1\ to\ 5$) as indicated in Equations 5 and 6.

$$\max_{0 \le \alpha_{i,j,m} \le 1} \left| correlation\left(\mathrm{WCI}_{i,j}, Qobs_k\right)\right| \tag{5}$$

For instance, for TSA/SST index ($i = 1$) and the first 3 months JFM ($j = 1$), the three-monthly weighted mean is:

$$\mathrm{WCI}_{1,1} = \frac{\alpha_{1,1,1} * \frac{\mathrm{TSA}}{\mathrm{SST}Jan} + \alpha_{1,1,2} * \frac{\mathrm{TSA}}{\mathrm{SST}Feb} + \alpha_{1,1,3} * \frac{\mathrm{TSA}}{\mathrm{SST}Mar}}{\alpha_{1,1,1} + \alpha_{1,1,2} + \alpha_{1,1,3}}, \tag{6}$$

After determining the coefficient $\alpha_{i,j,m}$, the Spearman correlation test was applied to $\mathrm{WCI}_{i,j}$ and $Qobs_k$ and the results were interpreted at 10% significance level.

2.4 | Flood discharge forecasting using climate indexes

A significant correlation between weighted climate indexes and flood time series of a given station suggests that its annual maximal discharge series can be approximated using a linear function of the weighted climate indexes. Therefore, flood peaks $Qsim_{i,j,k}$ were estimated as follows:

$$Qsim_{i,j,k} = a_k * \mathrm{WCI}_{i,j} + b_k \tag{7}$$

The regression coefficients a_k and b_k and the weights $\alpha_{i,j,m}$ (see Equation 6) were estimated by minimizing the difference between $Qsim_{i,j,k}$ and $Qobs_k$ using the Kling-Gupta Efficiency (*KGE*) (Gupta et al., 2009). Depending on the flood season identified for each station, $(T - j)$ corresponds to the lead time of the seasonal forecast with T the starting month of the flood season.

After assessing the flood predictability skill of each climate index, the forecast skill of combined climate indexes was evaluated using multiple linear regression analysis. The predictors considered are the three-month moving averages of each of the six climate indexes and the simulated discharge from the multiple linear regression, Qsim, is calculated as:

$$\mathrm{Qsim} = \sum_{i=0}^{6} a_i * WCI_i + b \tag{8}$$

with a_i and b the parameters to be identified by optimizing the KGE of Qsim and the corresponding Qobs. WCI_i corresponds to the three-month moving averages of each of the six climate indexes. The independence of the climate indexes used in the multiple linear regression was checked based on the variance inflation factor which was less than 10 for the selected indexes (Thompson et al., 2017).

2.5 | Forecast skill evaluation

The skill of a seasonal forecasting scheme to anticipate the right category of an event several months ahead is of great importance for decision-makers and flood risk managers (Gobena & Gan, 2010). For that purpose, the ability of the method for forecasting above normal and below normal annual maximal discharge was assessed using the ROC and the ROL after Mason and Graham (1999). The thresholds used for ROC and ROL computation were the lower and upper terciles of the observed annual maximal discharge (Thomson et al., 2006; Winsemius et al., 2014). We define as normal the range between the lower and upper terciles of the observed annual maximal discharge. The knowledge that flood magnitude for the coming season will be below normal (lower tercile) can guide reservoir managers in leaving less volume for flood control and subsequently store more water for irrigation and other usages. On the contrary, information on the above-normal flood for the coming season can guide dam water release strategies. For each station and lead time, a two-by-two contingency table for the verification of a binary forecast system was constructed and the following quantities were computed (Table 1).

$$\text{Hit rate}: HR = h/(h+m), \tag{9}$$

$$\text{False alarm rate}: FAR = \frac{f}{f+c}, \tag{10}$$

The hit and false-alarm rates, respectively, indicate the proportion of events for which a warning was provided adequately and the proportion of nonevents for which a warning was provided incorrectly (Mason & Graham, 1999). A receiver operating characteristic curve,

TABLE 1 Two-by-two contingency table for the verification of a binary forecast system

	Forecasts		
Observation	**Warning (W)**	**No warning (W′)**	**Total**
Event (E)	h	m	e
Nonevent (E′)	f	c	e′
Total	w	w′	n

Note: H refers to the number of times a flood warning was issued and was effectively observed; m is the number of times a flood event was not issued but was observed. The other quantities can be interpreted similarly.

or ROC curve, is a graphical plot that illustrates the diagnostic ability of a binary classifier system as its discrimination threshold varies. From the hit and false-alarm rates, the ROC score was calculated for each station and each lead time with a ROC score greater than 0.5 indicating a positive skill. The ROC score is usually calculated by plotting the hit rates against the false-alarm rates for different warning criteria and then inferring the area under the curve. A transformation of the ROC score was used so that it ranges from −100 (a perfectly bad forecasting system) to 100 (a perfect forecasting system) with 0 implying no skill, that is, same skill as the average observed annual maximal discharge:

$$ROC\ Score\ (\%) = 2 * (\text{ROC score} - 0.5) * 100 \quad (11)$$

The correct-alarm ratio indicates the proportion of times that an event occurred given that a warning had been provided while the miss ratio indicates the proportion of times an event occurred when no warning had been provided:

$$\text{Correct} - \text{alarm ratio}: CAR = h/(h+f), \quad (12)$$

$$\text{Miss ratio}: MR = m/(m+c) \quad (13)$$

Similar to ROC, the ROL score was calculated and was expressed as a percentage. ROC and ROL scores are two-dimensional measures of classification performance. For more information on ROC and ROL scores, the reader can refer to Mason and Graham (1999).

3 | RESULTS

3.1 | Data screening

Discharge data availability for West African river basins is very challenging. In total, the data of 150 discharge-gauging stations were obtained from GRDC and the national hydrological services mainly for the Niger, the Volta, and the Ouémé basins. The earliest record starts in 1922 (Tile-Mbeya, Nantaka, Koulikoro stations located in the Niger basin), while the most recent record ends in 2017 (Bonou station in the Ouémé basin). The 56 discharge stations having a minimum of 30 years data length were selected (Figure 2).

3.2 | Flood seasonality

The knowledge of flood timing, that is, the period when floods occur, is key information for flood risk reduction, water planning, and reservoir management. Flood occurrence in West Africa and the associated standard deviation are displayed in Figure 3. In general, floods occur within the 34th and the 46th week of the year (August to November) with some spatial discrepancies. Flood season in the upper and lower Niger varies between the 36th and 40th week of the year corresponding nearly to September to early October. In the middle Niger (upper closed curve in Figure 3), the mean flood timing varies between the 34th and the 46th week. The ITCZ movement governing rainfall onset, duration and amount, may explain this high variability of flood timing over the region. Earlier flood occurrence in the lower Niger compared to some parts of the middle Niger can be explained by the local rainfall regime leading to peak discharge greater than peak discharge associated with flows coming from the farthest tributaries in the Sahel (Badou et al., 2017; Le Barbé et al., 1993).

In the Volta-Mono-Couffo-Ouémé basins, the mean of flood timing varies between the 34th and 40th week (August to early October). This finding is in line with Fichì and Stephens (2019) who obtained similar results in northern sub-Saharan Africa (including the Sahel and Guinea region).

The results presented in Figure 3 suggest that the pre-flood season (period preceding flood season) ends in July. For the sake of simplicity, a homogeneous end of the pre-flood season namely week 30, was used for all catchments, despite the variation. This endpoint allows at least a 1-month lead time which is long enough to take necessary decisions to reduce flood impacts.

3.3 | Relationship between annual maximal discharge and climate indexes

The association between annual maximal discharge and climate indexes, weighted to three-month means, was evaluated with the Spearman correlation and tested at the 10% significance level (Figure 4). Positive as well as

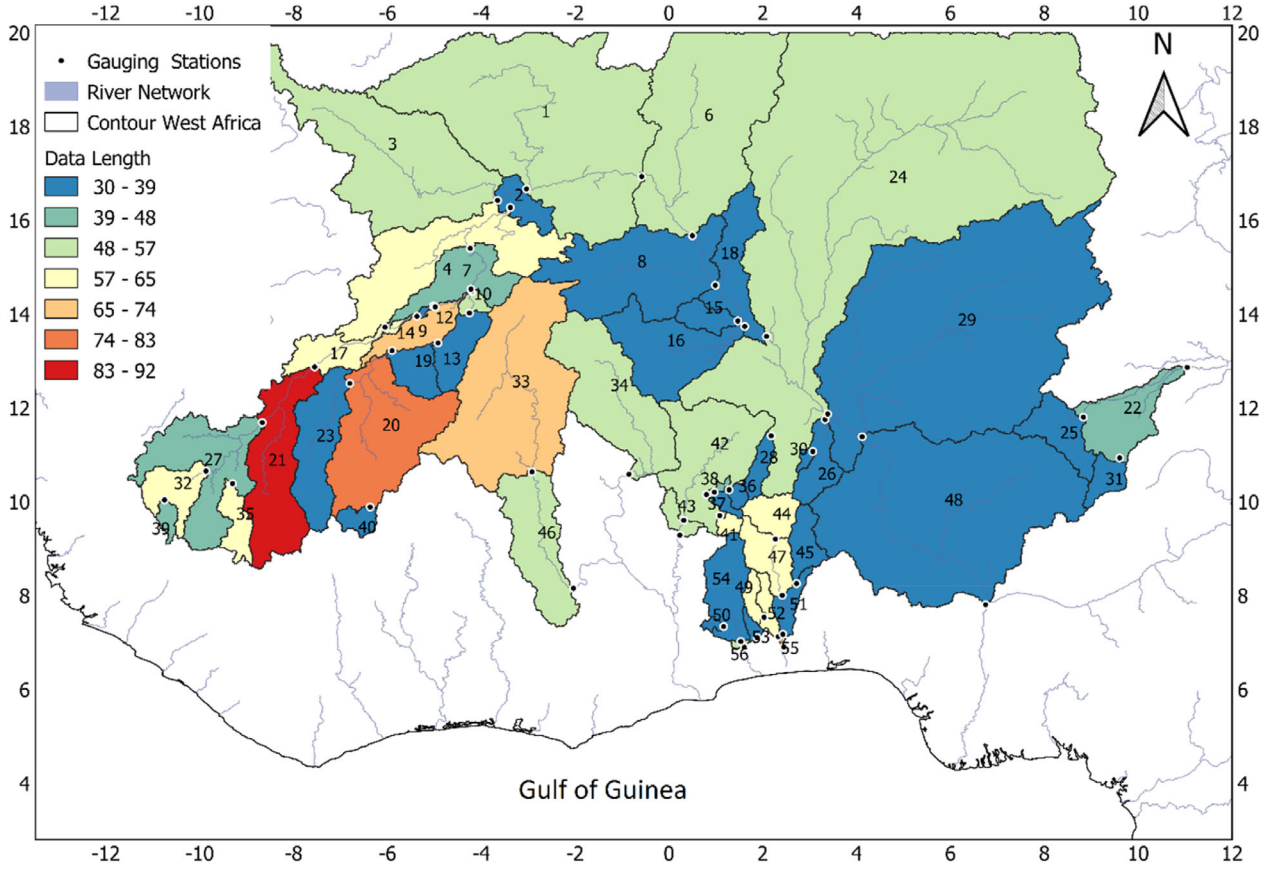

FIGURE 2 Location of stations, catchment boundaries and river network. Colors indicate available data length. Numbers refer to the station names given in Table S1 in the supplementary material

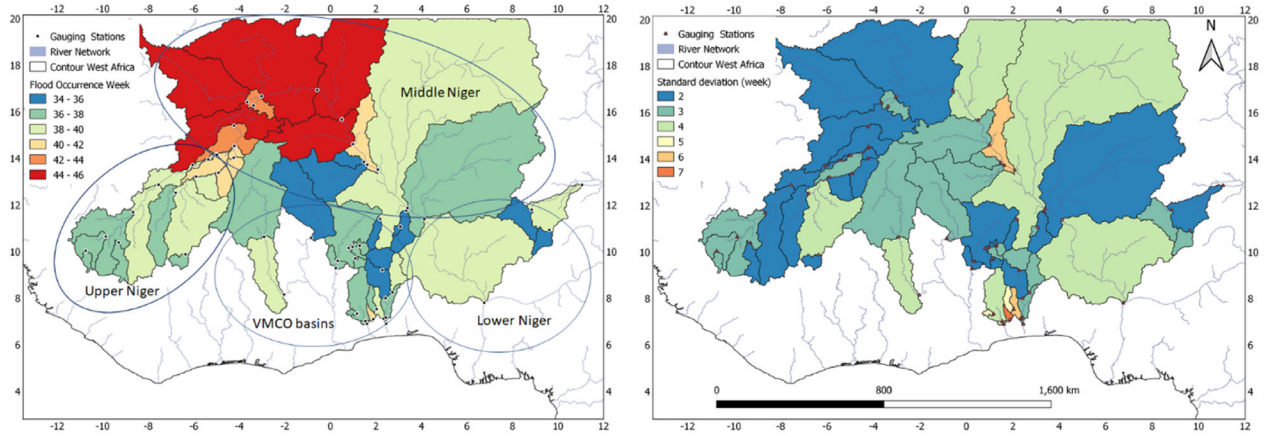

FIGURE 3 Week of flood occurrence (left) and the associated standard deviation (right) in West Africa. The closed curves on the left figure indicate the subdivision of the study area in four zones namely the upper, middle, and lower Niger, and the Volta-Mono-Couffo-Ouémé basins (basins)

negative correlations were found. SOI/SLP shows a mainly positive correlation, while the correlation of DMI_West/SST is primarily negative. Consistent correlations across different catchments and lead times are found for SOI/SLP and DMI_West/SST suggesting their substantial linkage to floods occurrence and magnitude in West Africa. This suggestion is supported by the high influence of DMI_West/SST (Atiah et al., 2020) and SOI/SLP (Egbuawa et al., 2017) on rainfall in West Africa. Therefore, the two climate indexes are promising predictors for seasonal forecasting of annual maximal discharge in the region.

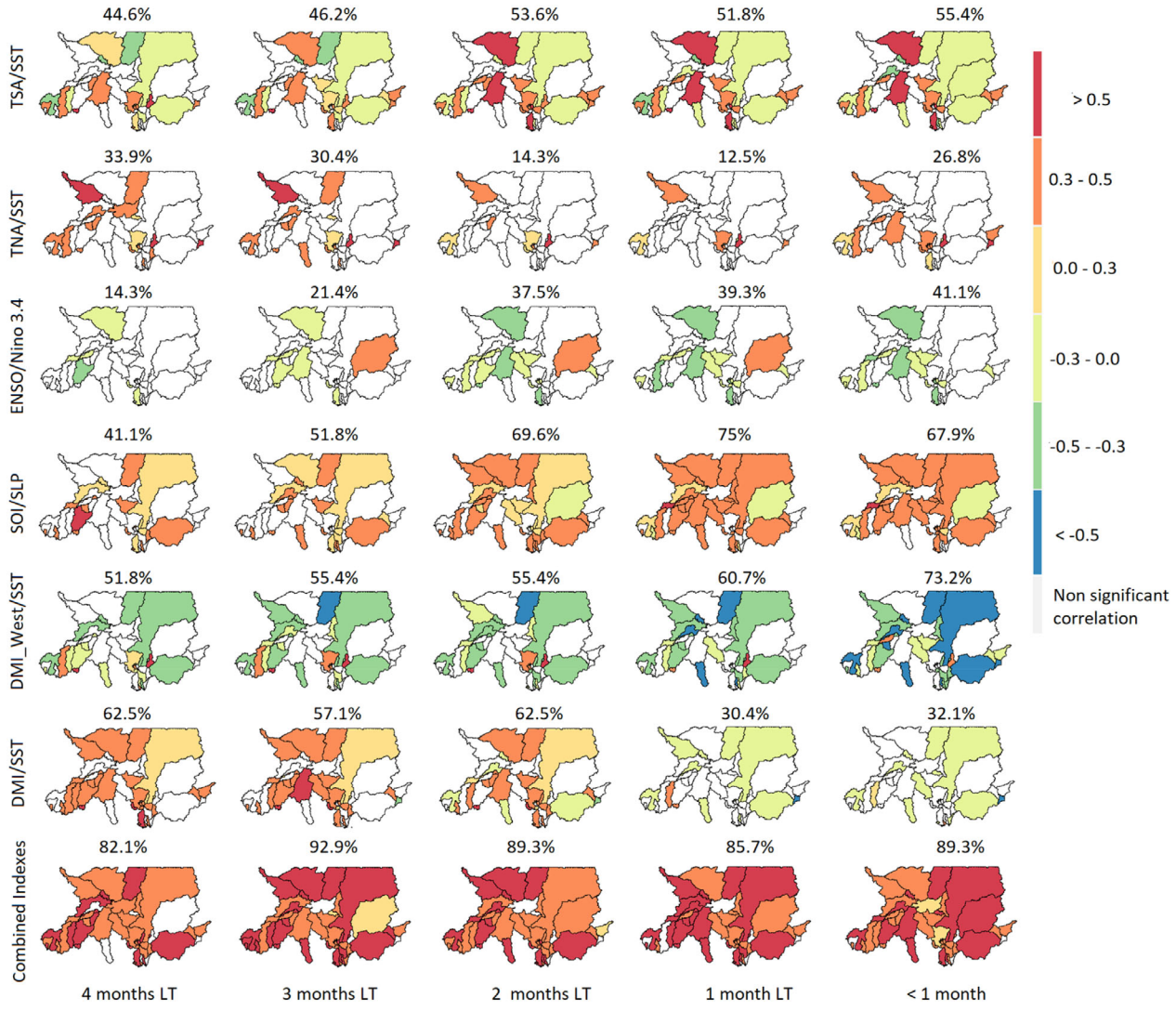

FIGURE 4 Statistically significant correlation coefficients between the annual maximal discharge and weighted three-month mean climate indexes. Values above each map indicate the percentage of stations showing a statistically significant correlation at 10%. SST refers to sea surface temperature, SLP is sea level pressure. TSA and TNA are the tropical southern Atlantic and tropical northern Atlantic indexes, respectively. ENSO/Nino3.4 is the SST anomaly in Nino 3.4 region. DMI is the dipole mode index and DMI_West is the western DMI of the equatorial Indian Ocean. Combined indexes refer to linear multiple regression of all indexes

TNA/SST shows a significant correlation with Qobs for a very limited number of stations scattered throughout the region with both highly variable positive and negative correlations depending on catchments and lead times. This suggests that TNA/SST is not a useful predictor for flood magnitude in West Africa. DMI/SST shows mainly positive and high correlations for lead times 2–4 months, but negative correlations for lead times equal to and smaller than 1 month.

A high and statistically significant correlation between Qobs of a given station and a climate index implies that the climate index can be used as a proxy for obtaining useful information about floods for the coming season. With the flood season spanning from August to November in West Africa, and in case of significant correlation, the three-month weighted mean climate indexes of JFM, FMA, MAM, AMJ, and MJJ would be valid predictors for flooding with corresponding lead times from 4 to 0 months. For the lead times of 4 and 3 months (JFM and FMA), DMI/SST shows the highest fractions of stations with significant correlations of 62.5% and 57.1%, respectively. For 2 and 1 months (MAM, AMJ), SOI/SLP gives the highest fractions with 69% and 75%, respectively. DMI_West/SST shows the highest number of stations (73.2%) with a significant correlation for the lead time of less than one month (MJJ). Overall, DMI_West/SST is the best individual climate index indicating a significant correlation with at least 52% of the stations,

irrespective of the lead time, followed by SOI/SLP (at least 41%).

The combination of all climate indexes through multiple linear regression outperformed the individual indexes in terms of the number of stations indicating a statistically significant correlation irrespective of lead-time. The strictly positive correlation found for all the stations confirmed that these covariates have the same influence on flood characteristics in the region and could serve as valid predictors. Due to the relatively low performance of TNA/SST and ENSO/Nino 3.4, they were excluded as potential individual predictors but considered in the multiple linear regression analysis.

3.4 | Flood predictability from climate indexes

The significant correlation between Qobs and climate indexes suggests that Qobs can be written as a linear function of these climate indexes. As shown in Figure 5, climate indexes are skillful indicators for predicting whether Qobs

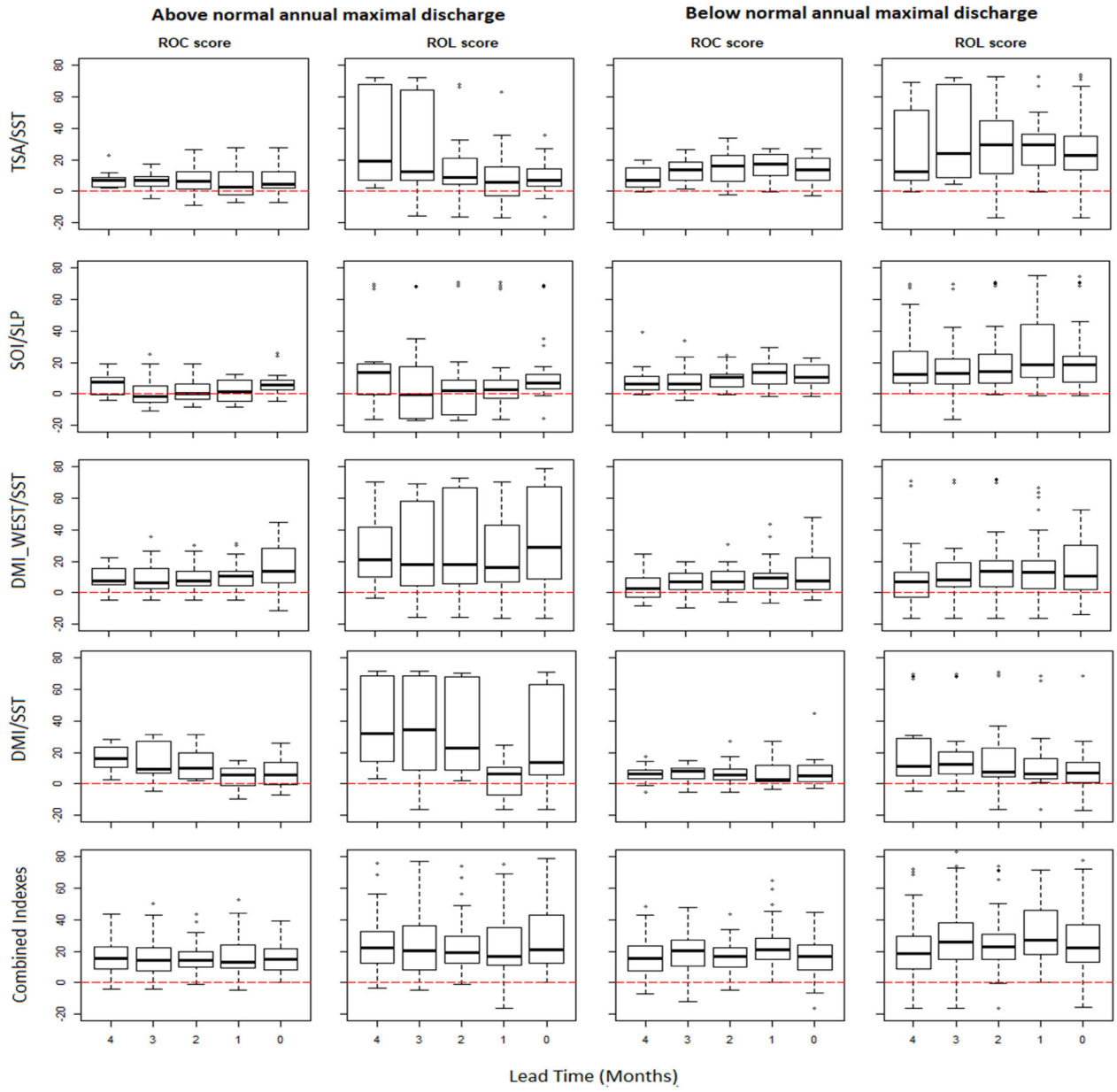

FIGURE 5 Boxplot of the ROC and ROL scores across the 56 stations for above normal and below normal annual maximal discharge and different lead times. SST refers to sea surface temperature, SLP is sea level pressure. TSA and TNA are the tropical southern Atlantic and tropical northern Atlantic indexes, respectively. DMI is the dipole mode index and DMI_West is the western DMI of the equatorial Indian Ocean. Combined indexes refer to linear multiple regression of all indexes

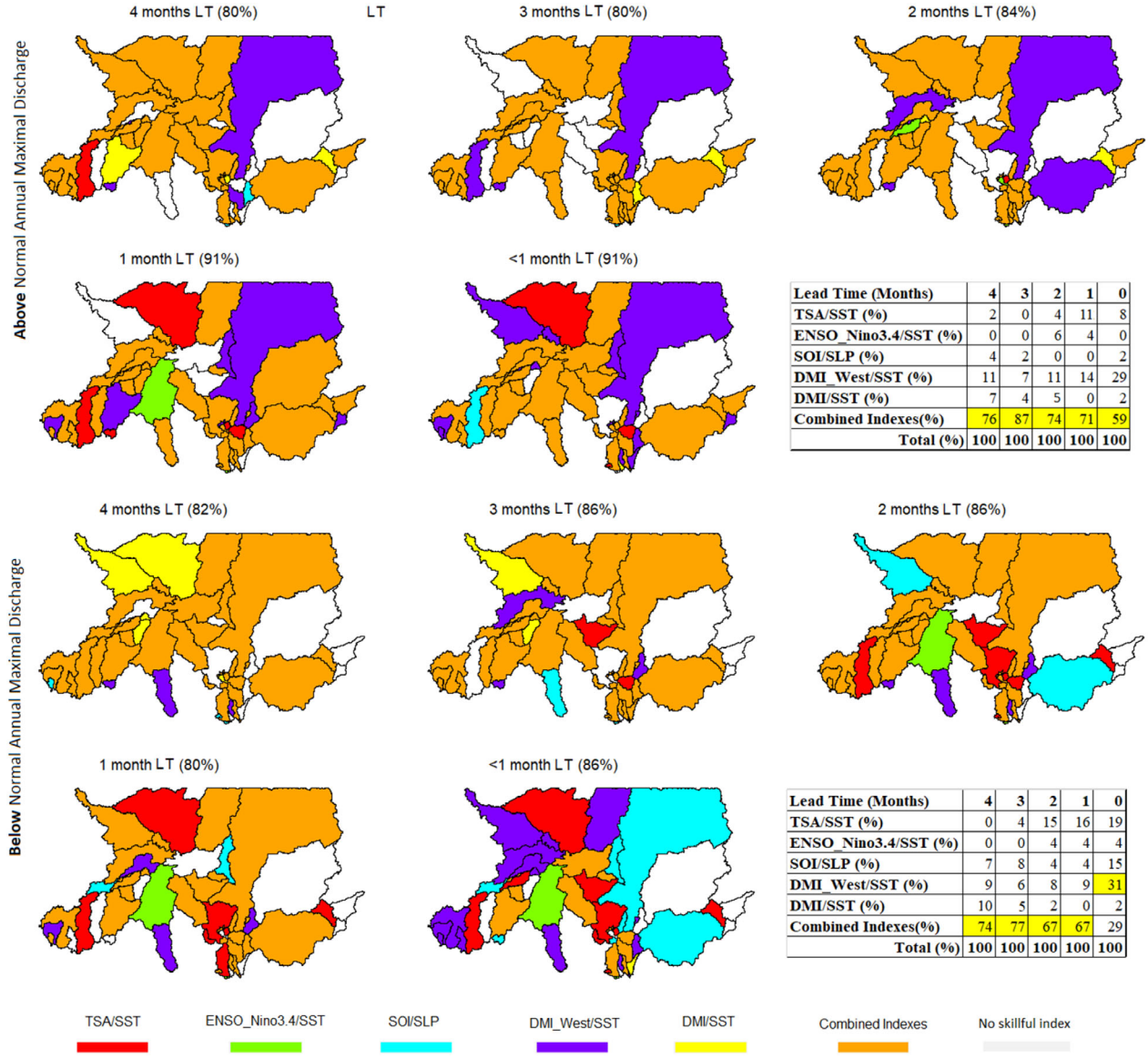

FIGURE 6 Best climate index for above (top rows) and below (bottom rows) normal flood prediction for each catchment and lead time. Numbers in brackets give the percentage of stations with positive skills using the best climate index. Tables display the percentage of stations with a positive skill for the different climate indexes and cells with yellow color indicate the best indexes. SST refers to sea surface temperature, SLP is sea level pressure. TSA and TNA are the tropical southern Atlantic and tropical northern Atlantic indexes, respectively. DMI is the dipole mode index and DMI_West is the western DMI of the equatorial Indian Ocean. Combined indexes refer to linear multiple regression of all indexes

in the coming months will be anomalously low or high. This is shown through the positive interquartile values of the ROC and the ROL scores for most of the lead times and climate indexes considered except SOI/SLP. A positive ROC score indicates that the hit rates, which provide an estimate of the probability that an event will be forecasted, are larger than false-alarm rates, which is the probability that for a nonevent a warning will be provided incorrectly (Mason & Graham, 1999). A positive ROL score implies that the correct-alarm ratio is greater than the miss ratio.

SOI/SLP and TSA/SST better predict below normal flood discharge as their median ROC scores are higher for below normal floods compared to above normal floods. In contrast, DMI/SST and DMI_West/SST better predict above normal flood discharge than below normal discharge. The median values of the ROL score are constantly greater than the corresponding median values of the ROC score for below and above normal discharge conditions. This implies that the ROC score tends to penalize the forecast system more than the ROL score. However, the performances indicated by the ROC score and ROL score are concordant.

For the above-normal discharge condition, the median ROC score using DMI_West/SST increases as the

lead time decreases, implying that as the flood season is approaching the performance of the prediction increases. In contrast to DMI_West/SST, the performance of predicting above-normal discharge using DMI/SST decreases as the flood season approaches. For below normal discharge, the performance using TSA/SST, SOI/SLP and DMI_West/SST, respectively, generally increases as the lead time decreases.

The combination of the six climate indexes through multiple linear regression maximizes the forecast skill as indicated by the strictly positive interquartile values of ROC and ROL score for below as well as for above normal annual maximal discharge regardless of the lead time. Hence, although the forecast performance varies for below and above normal flooding, the forecast system based on climate indexes has substantial skill in predicting below or above normal flooding up to 4 months ahead of the flood season.

The most skillful climate index for above or below normal flood prediction for each catchment and lead time is displayed in Figure 6. The percentage of catchments exhibiting positive skills for forecasting above normal floods generally increases with decreasing lead time, from 80% for 4 months to 91% for 1 month or less. For below normal floods, there is no general pattern. The forecasting system tends to be similarly skillful in predicting below normal flood discharge as well as above normal flooding.

The combined climate index shows the highest skill in forecasting both above and below normal floods in West Africa for almost all lead times. It is the best index for more than 70% of the skillful catchments for lead times greater than or equal to 1 month. For lead time less than 1 month, DMI_West/SST is the best climate index for 29% and 31% of the skillful catchments for above and below normal floods, respectively.

4 | DISCUSSIONS AND CONCLUSIONS

The potential usefulness of a seasonal forecasting system to predict above or below normal flood discharge in West Africa was assessed. The forecasts are based on simple and multiple linear relationships between observed annual maximal discharge (Qobs) and climate indexes for statistically significant correlations at the 10% significance level. Except for TNA/SST and ENSO_Nino3.4/SST, the four other climate indexes (TSA/SST, SOI/SLP, DMI_West/SST, and DMI/SST) indicated statistically significant correlations with Qobs for most of the catchments considered. The mainly positive correlations found for DMI/SST are in line with Dyer et al. (2017) who indicated that warming in the Indian Ocean induces an increase in the Sahelian rainfall while the opposite implies a decrease in the Sahelian rainfall. Extreme precipitation in the Sahel and Guinean coastal region, a proxy of high discharge, were found to be highly related with El Niño 3.4 index (Diatta et al., 2020) and, El Niño-Southern Oscillation (ENSO) and Mediterranean variability (Diakhaté et al., 2019), and Atlantic Ocean SST (Atiah et al., 2020). The combination of climate indexes in a linear multiple regression analysis significantly improved the prediction skill compared to individual climate indexes.

The potential differences in the results presented above due to the change in the significance level from 10% to 5% for correlation analysis were tested. For that purpose, all the correlation analyses between the three-month weighted mean climate indexes and the observed annual maximal discharge have been repeated using the 5% significance level. For the combined climate indexes, the correlation was computed between the simulated annual maximal discharge from the multiple linear regression and the observed annual maximal discharge. The results of the percentage change between the number of stations indicating statistically significant correlation at 10% and 5% levels are shown in Table S2 in the supplementary material. When considering single climate indexes, it can be observed that from 10% to 5% significance levels, the results substantially differ with a decrease in the number of statistically significant stations between 12 to 75%. However, for the multiple linear regression based on all the indexes, the difference between the two outputs is less than 10%. This indicates that the multiple linear regression model which outperformed the models based on individual indexes (see ROC and ROL scores) is not very sensitive to the variation in the significance levels from 10 to 5%.

While the linkage between extreme precipitation and climate indexes has been widely investigated in West Africa, knowledge about teleconnections between flood characteristics and climate indexes is very limited. Our study is among the first to investigate the climate-flood link in West Africa. In a global study, Ward, Jongman, et al. (2014) found a strong linkage between ENSO and parts of the Sahel and western Africa flood risk. Li et al. (2016) analyzed flood events for 55 countries in Africa relative to ENSO (SOI) years and found a statistically significant relationship at a continental level. A strong linear correlation between annual discharges and ENSO was also found in South Africa (Alemaw & Chaoka, 2006) and the Nile river basin (Siam & Eltahir, 2015). Hence, our study is the first study to explore the relationship between floods and climate for other climate modes besides ENSO.

The potential benefits of flood forecasting increase with the forecast lead time. The forecasting skill was evaluated

using the ROC and ROL scores by considering the lower and upper terciles as reference thresholds (Arnal et al., 2018; Mason & Graham, 1999). According to the ROC score, most of the forecasting models mainly the multiple linear regression model were skillful compared to the perpetual warnings or no warnings situation (Mason & Graham, 1999), corresponding to the average historical hydrometeorological information. It can provide useful information on the coming flood season up to 4 months ahead.

The forecast models are based on a direct (and linear) relationship between flood peaks and climate indexes. This link does not consider a range of processes, such as flood-triggering rainfall patterns, antecedent catchment state, run-off generation, and human interventions in catchments and rivers that modulate the relation between large-scale climate indexes and local flood characteristics. However, as the forecasting models are completely based on observations, these processes are inherently embedded in the models–at least in a rough way.

Despite their simplicity, the forecasting models showed positive skill, compared to the average hydrometeorological situation, for lead times of up to 4 months. Such a long period can be of large value for decision-making. The forecasts of above-normal flood discharge, several months ahead, can help alert agencies and the public of entering a period of an increased chance of flooding and therefore improve flood preparedness for the upcoming flood season. It would be interesting to explore how the identified links between climate variability and streamflow could be exploited for flood risk management but also for other water-related sectors, such as water resources management (White et al., 2017), hydropower generation (Lima & Lall, 2010), and dam management (Viel et al., 2016).

ACKNOWLEDGEMENTS

This work has been funded by the DAAD under the ClimapAfrica program.

DATA AVAILABILITY STATEMENT

The data that support the findings of this study are available on request from the corresponding author. The data are not publicly available due to privacy or ethical restrictions.

ORCID

Jean Hounkpè https://orcid.org/0000-0002-5521-9339
Bruno Merz https://orcid.org/0000-0002-5992-1440
Félicien D. Badou https://orcid.org/0000-0001-5159-7095
Yacouba Yira https://orcid.org/0000-0003-3879-8153
Emmanuel A. Lawin https://orcid.org/0000-0003-4751-3439

REFERENCES

Aguilar, C., Montanari, A., & Polo, M. J. (2017). Real-time updating of the flood frequency distribution through data assimilation. *Hydrology and Earth System Sciences*, *21*(7), 3687–3700. https://doi.org/10.5194/hess-21-3687-2017

Alemaw, B. F., & Chaoka, T. R. (2006). The 1950-1998 warm ENSO events and regional implications to river flow variability in southern Africa. *Water, SA*, *32*, 459–464. https://orcid.org/10.4314/wsa.v32i4.5153

Arnal, L., Cloke, H. L., Stephens, E., Wetterhall, F., Prudhomme, C., Neumann, J., Krzeminski, B., & Pappenberger, F. (2018). Skilful seasonal forecasts of streamflow over Europe? *Hydrology and Earth System Sciences*, *22*(4), 2057–2072. https://doi.org/10.5194/hess-22-2057-2018

Atiah, W. A., Mengistu Tsidu, G., Amekudzi, L. K., & Yorke, C. (2020). Trends and interannual variability of extreme rainfall indices over Ghana, West Africa. *Theoretical and Applied Climatology*, *140*(3–4), 1393–1407. https://doi.org/10.1007/s00704-020-03114-6

Bayliss, A. C., & Jones, C. R. (1993). Peaks-over-threshold flood database: Summary statistics and seasonality. https://nora.nerc.ac.uk/id/eprint/6075/1/IH_121.pdf

Badou, D. F., Kapangaziwiri, E., Diekkrüger, B., Hounkpè, J., & Afouda, A. (2017). Evaluation of recent hydro-climatic changes in four tributaries of The Niger River basin (West Africa). *Hydrological Sciences Journal*, *62*(5), 715–728. https://doi.org/10.1080/02626667.2016.1250898

Blöschl, G., Hall, J., Parajka, J., Perdigão, R. A. P., Merz, B., Arheimer, B., Aronica, G. T., Bilibashi, A., Bonacci, O., Borga, M., Čanjevac, I., Castellarin, A., Chirico, G. B., Claps, P., Fiala, K., Frolova, N., Gorbachova, L., Gül, A., Hannaford, J., ... Živković, N. (2017). Changing climate shifts timing of European floods. *Science*, *357*(6351), 588–590. https://doi.org/10.1126/science.aan2506

Chambers, J. M., Cleveland, W. S., Kleiner, B., & Turkey, A. P. (2018). *Graphical methods for data analysis*. Taylor & Francis Group.

CPC/NOAA. (2005). El Nino Southern Oscillation Index. https://www.cpc.ncep.noaa.gov/products/analysis_monitoring/ensostuff/detrend.nino34.ascii.txt

Diakhaté, M., Rodríguez-Fonseca, B., Gómara, I., Mohino, E., Dieng, A. L., & Gaye, A. T. (2019). Oceanic forcing on interannual variability of Sahel heavy and moderate daily rainfall. *Journal of Hydrometeorology*, *20*(3), 397–410. https://doi.org/10.1175/JHM-D-18-0035.1

Diatta, S., Diedhiou, C. W., Dione, D. M., & Sambou, S. (2020). Spatial variation and trend of extreme precipitation in west africa and teleconnections with remote indices. *Atmosphere*, *11*(9), 1: 23. https://doi.org/10.3390/atmos11090999

Dottori, F., Szewczyk, W., Ciscar, J., Zhao, F., Alfieri, L., Hirabayashi, Y., Bianchi, A., Mongelli, I., Frieler, K., Betts, A. R. & Feyen, L. (2018). Increased human and economic losses from river flooding with anthropogenic warming. *Nature Climate Change.*, *8*, 781–786. https://doi.org/10.1038/s41558-018-0257-z

Dyer, E. L. E., Jones, D. B. A., Li, R., Sawaoka, H., & Mudryk, L. (2017). Sahel precipitation and regional teleconnections with the Indian Ocean. *Journal of Geophysical Research*, *122*(11), 5654–5676. https://doi.org/10.1002/2016JD026014

Egbuawa, O. I., Anyanwu, J. C., Amaku, G. E., & Onuoha, I. C. (2017). Assessment of the teleconnection between El Nino

southern oscillation (ENSO) and west African rainfall. *African Research Review*, *11*(4), 17. https://doi.org/10.4314/afrrev.v11i4.3

Enfield, D. B., Mestas, A. M., Mayer, D. A., & Cid-Serrano, L. (1999). How ubiquitous is the dipole relationship in tropical Atlantic sea surface temperatures? *JGR-O*, *104*, 7841–7848. https://doi.org/10.1029/1998JC900109

Ficchì, A., & Stephens, L. (2019). Climate variability alters flood timing across Africa. *Geophysical Research Letters*, *46*(15), 8809–8819. https://doi.org/10.1029/2019GL081988

Gobena, A. K., & Gan, T. Y. (2010). Incorporation of seasonal climate forecasts in the ensemble streamflow prediction system. *Journal of Hydrology*, *385*(1–4), 336–352. https://doi.org/10.1016/j.jhydrol.2010.03.002

Gupta, H. V., Kling, H., Yilmaz, K. K., & Martinez, G. F. (2009). Decomposition of the mean squared error and NSE performance criteria: Implications for improving hydrological modelling. *Journal of Hydrology*, *377*, 80–91. https://doi.org/10.1016/j.jhydrol.2009.08.003

Hounkpè, J., Diekkrüger, B., Badou, D., & Afouda, A. (2015). Non-stationary flood frequency analysis in the Ouémé River basin, Benin Republic. *Hydrology*, *2*(4), 210–229. https://doi.org/10.3390/hydrology2040210

Kiem, A. S., Franks, S. W., & Kuczera, G. (2003). Multi-decadal variability of flood risk, *30*(2), 1–4. https://doi.org/10.1029/2002GL015992

Kundzewicz, Z. W., Szwed, M., & Pińskwar, I. (2019). Climate variability and floods-A global review. *Water (Switzerland)*, *11*(7), 1:24. https://doi.org/10.3390/w11071399

Le Barbé, L., Alé, G., Millet, B., Texier, H., Borel, Y., & Gualde, R. Les ressources en eaux superficielles de la République du Bénin (1993). http://www.hydrosciences.fr/sierem/produits/biblio/Monographies/N°11-Monographie

Li, C., Chai, Y., & Yang, L. (2016). Spatio-temporal distribution of flood disasters and analysis of influencing factors in Africa. *Natural Hazards*, *82*(1), 721–731. https://doi.org/10.1007/s11069-016-2181-8

Lima, C. H. R., & Lall, U. (2010). Climate informed long term seasonal forecasts of hydroenergy inflow for the Brazilian hydropower system. *Journal of Hydrology*, *381*(1–2), 65–75. https://doi.org/10.1016/j.jhydrol.2009.11.026

Mason, S. J., & Graham, N. E. (1999). Conditional probabilities, relative operating characteristics, and relative operating levels. *Weather and Forecasting*, *14*(5), 713–725. https://doi.org/10.1175/1520-0434(1999)014<0713:CPROCA>2.0.CO;2

Merz, B., Blöschl, G., Vorogushyn, S., Dottori, F., Aerts, J. C. J. H., Bates, P., Bertola, M., Kemter, M., Kreibich, H., Lall, U., & Macdonald, E. (2021). Causes, impacts and patterns of disastrous river floods. *Nature Reviews Earth & Environment*, *592–609*, 592–609. https://doi.org/10.1038/s43017-021-00195-3

Nakamura, J., Lall, U., Kushnir, Y., Robertson, A. W., & Seager, R. (2013). Dynamical structure of extreme floods in the U. S. midwest and the United Kingdom. *Journal of Hydrometeorology*, *14*, 485–505. https://doi.org/10.1175/JHM-D-12-059.1

NOAA. (2020). Linear Correlations in Atmospheric Seasonal/Monthly Averages. https://psl.noaa.gov/data/correlation/tna.data, https://psl.noaa.gov/data/correlation/tsa.data

NOAA. (2021). (STAND TAHITI - STAND DARWIN) SEA LEVEL PRESS ANOMALY. https://www.cpc.ncep.noaa.gov/data/indices/soi

Räsänen, T. A., & Kummu, M. (2013). Spatiotemporal influences of ENSO on precipitation and flood pulse in the Mekong River basin. *Journal of Hydrology*, *476*, 154–168. https://doi.org/10.1016/j.jhydrol.2012.10.028

Siam, M. S., & Eltahir, E. A. B. (2015). Explaining and forecasting interannual variability in the flow of the Nile River. *Hydrology and Earth System Sciences*, *19*(3), 1181–1192. https://doi.org/10.5194/hess-19-1181-2015

Smith, C. (2020). Dipole Mode Index (DMI). https://psl.noaa.gov/gcos_wgsp/Timeseries/DMI/

Steirou, E., Gerlitz, L., Apel, H., Sun, X., & Merz, B. (2019). Climate influences on flood probabilities across Europe. *Hydrology and Earth System Sciences*, *2014*, 1305–1322. https://doi.org/10.5194/hess-23-1305-2019

Thiemig, V., de Roo, A., & Gadain, H. (2011). Current status on flood forecasting and early warning in Africa. *International Journal of River Basin Management*, *9*(1), 63–78. https://doi.org/10.1080/15715124.2011.555082

Thompson, C. G., Kim, R. S., Aloe, A. M., & Becker, B. J. (2017). Extracting the variance in flation factor and other multicollinearity diagnostics from typical regression results. *Basic and Applied Social Psychology*, *39*(2), 81–90. https://doi.org/10.1080/01973533.2016.1277529

Thomson, M. C., Mason, S. J., Hagedorn, R., Connor, S. J., Phindela, T., Morse, A. P., & Palmer, T. N. (2006). Malaria early warnings based on seasonal climate forecasts from multi-model ensembles. *Nature Letters*, *439*, 576. https://doi.org/10.1038/nature04503

Viel, C., Beaulant, A.-L., Soubeyroux, J.-M., & Céron, J.-P. (2016). How seasonal forecast could help a decision maker: An example of climate service for water resource management. *Advances in Science and Research*, *13*, 51–55. https://doi.org/10.5194/asr-13-51-2016

Ward, P. J., Eisner, S., Flörke, M., Dettinger, M. D., & Kummu, M. (2014). Annual flood sensitivities to El Niño–Southern oscillation at the global scale. *Hydrology and Earth System Sciences*, *18*, 47–66. https://doi.org/10.5194/hess-18-47-2014

Ward, P. J., Jongman, B., Kummu, M., Dettinger, M. D., Weiland, F. C. S., & Winsemius, H. C. (2014). Strong influence of El Niño southern oscillation on flood risk around the world. *Proceedings of the National Academy of Sciences of the United States of America*, *111*(44), 15659–15664. https://doi.org/10.1073/pnas.1409822111

Ward, P. J., van Pelt, S. C., de Keizer, O., Aerts, J. C. J. H., Beersma, J. J., & van den Hurk, B. J. J. M. (2014). Including climate change projections in probabilistic flood risk assessment. *Journal of Flood Risk Management*, *7*(2006), 141–151. https://doi.org/10.1111/jfr3.12029

White, C. J., Carlsen, H., Robertson, A. W., Klein, R. J. T., Lazo, J. K., Kumar, A., Vitart, F., Coughlan de Perez, E., Ray, A. J., Murray, V., Bharwani, S., MacLeod, D., James, R., Fleming, L., Morse, A. P., Eggen, B., Graham, R., Kjellström, E., Becker, E., … Zebiak, S. E. (2017). Potential applications of subseasonal-to-seasonal (S2S) predictions. *Meteorological Applications*, *24*(3), 315–325. https://doi.org/10.1002/met.1654

Winsemius, H. C., Dutra, E., Engelbrecht, F. A., & van Garderen, E. A. (2014). The potential value of seasonal forecasts in a changing climate. *Hydrology and Earth System Sciences*, *18*, 14747–14782. https://doi.org/10.5194/hessd-10-14747-2013

Zanardo, S., Nicotina, L., Hilberts, A. G. J., & Jewson, S. P. (2019). Modulation of economic losses from European floods by the North Atlantic oscillation. *Geophysical Research Letters*, *46*(5), 2563–2572. https://doi.org/10.1029/2019GL081956

SUPPORTING INFORMATION

Additional supporting information can be found online in the Supporting Information section at the end of this article.

How to cite this article: Hounkpè, J., Merz, B., Badou, F. D., Bossa, A. Y., Yira, Y., & Lawin, E. A. (2022). Potential for seasonal flood forecasting in West Africa using climate indexes. *Journal of Flood Risk Management*, e12833. https://doi.org/10.1111/jfr3.12833